Smart Agricultural Technology 7 (2024) 100428

Contents lists available at ScienceDirect

Smart Agricultural Technology

journal homepage: www.journals.elsevier.com/smart-agricultural-technology

Trunk dielectric permittivity correlates with irrigation based on soil water content in fruit trees

María R. Conesa [a,*], Juan Vera [a], Wenceslao Conejero [a], Virginia Hernandez-Santana [b], María Carmen Ruiz-Sánchez [a]

[a] Irrigation Department, Consejo Superior de Investigaciones Científicas (CSIC) Centro de Edafología y Biología Aplicada del Segura (CEBAS-CSIC), Campus de Espinardo, 25, 30100, Murcia, Spain

[b] Irrigation and Ecophysiology Group & Laboratory of Plant Molecular Ecophysiology. Instituto de Recursos Naturales y Agrobiología (IRNAS-CSIC), Avda Reina Mercedes, 10, 41012, Sevilla, Spain

ARTICLE INFO

Keywords:
Automatic soil-based irrigation system
Dielectric permittivity (k)
Management allowed depletion (MAD)
volumetric trunk water content ($\theta_{v\text{-}trunk}$)
TDR-305N
volumetric soil water content ($\theta_{v\text{-}soil}$)

ABSTRACT

Time-domain reflectometry (TDR) is an electromagnetic technique that measures the dielectric permittivity (K) which is a surrogate property influenced by water content. Advances in nanoelectronics have enabled the development of a TDR probe (TDR-305 N) to monitor changes in K, bulk electrical conductivity (EC_{bulk}) and temperature (T) in a porous medium, such as a tree trunk. The main objective of this study was to assess the effectiveness of the TDR-305 N sensors for real-time monitoring changes in water content in the trunk of nectarine trees. Throughout the summer of 2022, irrigation was automatically managed with threshold values of soil water content ($\theta_{v\text{-}soil}$) measured with capacitance probes. Different management allowed depletion (MAD) values were set to trigger irrigation: 50 % in July (moderate water deficit), 100 % in August (severe water deficit), and recovery to well-irrigated conditions in September. Discrete measurements of midday stem water potential ($\Psi_{s,md}$) and leaf gas exchange were made frequently. The results showed a progressive reduction of the measured physiological parameters, as well as of K and EC_{bulk} and $\theta_{v\text{-}soil}$ decreased. Notably, $\Psi_{s,md}$ reached a critically low value of -2.03 MPa, coinciding with pronounced and severe stomatal closure. Both K and $\Psi_{s,md}$, were able to explain the variations of $\theta_{v\text{-}soil}$ by more than 75 %. Daily, a positive relationship of K and EC_{bulk} was observed, although EC_{bulk} exhibited a stronger dependence on T_{trunk} compared to K. Furthermore, K did not return to its initial values prior to the onset of water stress, possibly influenced by xylem cavitation and a reduction in leaf area during its senescence stage. The findings suggest that trunk permittivity measurements obtained using TDR-305 N sensors could be a reliable indicator for monitoring tree water status. However, further research is needed to determine the threshold values of trunk water content under non-limiting soil water conditions for accurate irrigation scheduling.

Introduction

In Mediterranean agriculture, high production levels and fruit quality of crops depend on accurate and efficient irrigation regimes. Inadequate irrigation management can lead to water stress in plants due to deficit or excess irrigation, which can affect the quantity and quality of fruit at harvest. Drought is the most damaging stress that negatively affects plant productivity. Other factors, such as increasing urbanisation, population growth, or inequitable economic development itself, have contributed to increasingly intensive water use and thus to a higher risk of reaching more extreme levels of water stress in the short term. Furthermore, excessive irrigation is particularly associated with higher costs (both for the water used and the associated energy required) and generates significant nutrient losses through leaching, which can lead to environmental problems related to groundwater contamination and soil depletion [1,2].

Precision irrigation is a key factor in minimising production costs and pollution risks, as well as improving water productivity. It is based on the use of methodologies that measure water status in the soil-plant-atmosphere continuum [3]. Volumetric soil water content ($\theta_{v\text{-}soil}$) is often recommended as a crucial input for irrigation management decision support systems (DSS). Irrigation scheduling based on real-time

* Corresponding author.
E-mail address: mrconesa@cebas.csic.es (M.R. Conesa).

https://doi.org/10.1016/j.atech.2024.100428
Received 15 October 2023; Received in revised form 6 February 2024; Accepted 29 February 2024
Available online 3 March 2024

$\theta_{v\text{-}soil}$ helps to reduce the risks related to runoff, erosion, and groundwater pollution, while improving irrigation water productivity [4]. Due to their automation capability and high accuracy over a wide range of moisture content, dielectric soil sensors are the most advantageous method [5]. Capacitance probes have been widely used in automated drip irrigation systems due to their low cost, low energy consumption and reasonable accuracy [5,6]. In nectarine trees, the automated system managed with capacitance probes proposed by Conesa et al. [7] allowed water savings of about 40 % with no yield penalty compared to conventional irrigation scheduling by crop evapotranspiration (ETc, [8]). In plum trees, Millán et al. [9] established a regulated deficit irrigation strategy based on 40 % ETc modulated by capacitance soil moisture sensors in plum trees. In addition, the automated algorithm of Dominguez-Niño et al. [10] saved 23 % of the irrigation volume compared to the traditional water balance method.

Decisions on ON/OFF irrigation are typically based on the comparison of the measured soil water status with a certain preestablished threshold value [11]. Commonly, $\theta_{v\text{-}soil}$ is used as a threshold value, this is often considered as the field capacity (FC) or a derived value called management allowed depletion (MAD) that is defined as a fraction of the difference between the soil water content at FC and at the permanent wilting point (PWP). Therefore, MAD is the fraction of the soil total available water that can be depleted before plants experience water stress; thus, under a precision irrigation regime, an irrigation event is triggered ON each time the soil water content declines down to the value of (FC-MAD) [12]. Automatic Soil-based Irrigation System combines the information collected by a wireless sensor network (WSN) through a web platform, allowing real-time field data to be obtained, which operate the electro-valves using IoT technologies without human intervention. Furthermore, all recorded data is stored in the cloud and is available anywhere and anytime to end-users or farmers [2]. Real-time automated irrigation treatment fed with $\theta_{v\text{-}soil}$ threshold values, based on the MAD-concept, and combined with regulated deficit irrigation criteria [13], has demonstrated to be a successful irrigation strategy in field-woody crops experiments [7,14–19].

Assessing plant water status provides inputs to develop new water-saving irrigation strategies. Previously, plant water status was estimated indirectly through $\theta_{v\text{-}soil}$, but the physiological response of the plant to water deficit is essentially affected by changes in leaf and stem water content, rather than by highly variable soil water dynamics [20]. For this reason, plant-based approaches have proven to be more accurate and sensitive in estimating plant water status, especially in woody crops, as the deep nature of their root systems presents some difficulties in estimating soil moisture content [21,22].

Stem water potential monitoring at midday ($\Psi_{s,md}$) is an effective method for determining the water status of plants [23], but the method involves labour-intensive and destructive measurements and cannot be automated. In this regard, the new sensors identified as micro-tensiometers are able to continuously measure trunk water potential (Ψ_{trunk}), which is one of the main advantages compared to discrete determinations of $\Psi_{s,md}$. Recently, Conesa et al. [24] demonstrated that Ψ_{trunk} faithfully reveals the impact of automated MAD-based irrigation scheduling in nectarine trees.

Another method for estimating plant water status involves the assessment of plant water storage capacity, which is determined by the hydraulic capacitance of a plant tissue [25]. Within plants, trunk (or stem) water content ($\theta_{v\text{-}trunk}$) is one of the most common plant-based water indicators [26]. The tree trunk reveals substantial seasonal and diurnal variations in its water content because of transpiration fluxes [27]. Furthermore, $\theta_{v\text{-}trunk}$ is not only critical for supporting daily and seasonal transpiration, but is in turn related to tree photosynthesis, tree growth and the ability of trees to withstand drought stress period.

The Time Domain Reflectometry (TDR) technique measures the travel time of electromagnetic wave and determines the dielectric permittivity (K) of a porous material (*e.g.,* soil, wood…) [28]. K is a property that measures the ability of the material used to store energy when an electrical field is applied. The equation of Topp et al. [29] is the most widely used model to estimate $\theta_{v\text{-}soil}$ from K values with TDR sensors, being also extensible to other porous materials with appropriate calibration. Several researchers have inserted TDR and other electromagnetic sensors into the wood of trees to determine their water content, drawing attention to the way and position in which the sensor is installed in the trunk to obtain reliable data on instantaneous changes of $\theta_{v\text{-}trunk,}$ and their wounding effects [26].

Nadler et al. [30,31] noted that TDR was able to determine trunk hydration in lemon and mango, but the signal had too much noise and the system was too expensive to manage orchard irrigation. Furthermore, most of the literature on the use of TDR sensors to monitor plant water status had been conducted on forest trees [26,27,32,33], among others]. Therefore, there are still several challenges in determining $\theta_{v\text{-}trunk}$ using the TDR technique in fruit trees and using it to manage irrigation in fruit orchards.

This paper examines the capability of a TDR sensor, the TDR-305 N, as a non-destructive device to monitor changes in plant water status after insertion into the trunk of nectarine trees. It records instantaneous values of K and EC_{bulk}, which are essential for estimating $\theta_{v\text{-}trunk}$. Irrigation scheduling was automatically managed by real-time $\theta_{v\text{-}soil}$ values at different soil MAD levels corresponding to moderate and severe deficit, followed by a recovery irrigation period to meet crop water requirements. This study also analyses how K and EC_{bulk} trunk measurements can reveal the established automated soil-based irrigation protocol.

Material and methods

Orchard site description

This study was conducted during the postharvest period of 2022 (Day of the year, DOY 180–280) in a 0.5 ha orchard of 12-year-old early-maturing (harvested in May) nectarine trees (*Prunus persica* (L.) Batsch, cv. Flariba, grafted on GxN-15 rootstock) located at the CEBAS-CSIC experimental station, Santomera, Murcia (Spain). Nectarine trees were spaced 6.5 m x 3.5 m and trained to an open-centre canopy. The soil in the 0–50 cm layer was highly calcareous (45 % calcium carbonate), with a clay loam texture (clay fraction: 41 % illite, 17 % smectite, and 30 % palygorskite), low organic matter content (1.3 %), and a cation exchange capacity of 97.9 mmol kg^{-1}. The average bulk density was 1.43 g cm^{-3}. $\theta_{v\text{-}soil}$ at field capacity and at permanent wilting point was 0.29 and 0.14 m^3 m^{-3}, respectively.

The nectarine trees were drip irrigated with four emitters per tree with a nominal flow rate of 4 L h^{-1} inserted in a single drip line per row of trees. The emitters were located at 0.5 and 1.3 m both sides of the tree trunk.The irrigation water collected from the water distribution network of the Irrigation Community of Santomera called “Azarbe del Merancho” with an average electrical conductivity ($EC_{25^\circ C}$) of 0.8 dS m^{-1}. Annual fertilisation (83, 24 and 90 kg ha^{-1} of N, P and K, [34]) was applied through the irrigation system [35]. Standard cultural practices (*e.g.,* weed control, pruning and fruit thinning among others) were carried out by the technical personnel of the CEBAS-CSIC experimental station following local fruit growing practices.

Environmental data, including reference crop evapotranspiration (ET_0, [8]), air temperature (T_{air}) and relative humidity (RH) were recorded by an automated station located 0.25 km from the orchard, which read values every 5 min and recorded averages every 15 min, allowing the vapour pressure deficit (VPD) to be calculated.

The study consisted of an automated soil-based irrigation schedule system managed according to different decision criteria (see 2.2 section). Irrigated trees were distributed in a randomised complete block design with four replications. Each replication consisted of a row of six individual trees ($n = 24$). Measurements of soil and plant water relations were made on a representative tree from each replicate.

Automatic soil-based irrigation treatment

$\theta_{v\text{-}soil}$ was monitored with multi-depth EnviroScan® (Sentek Sensor Technologies, Sidney, Australia) capacitance probes. Four PVC access tubes were installed 0.1 m from the emitter located close (0.5 m) to the tree trunk in four trees (one per each replicate). Each capacitance probe had sensors at 0.1, 0.3, 0.5, and 0.7 m depth, and was connected to a radio transmission unit. Values were read every 5 min, and the average recorded every 15 min. The probes were normalized to maximum and minimum frequency readings in water and air respectively and then configured to use the calibration equation reported by Evett et al. [36] for a clay-loam soil. The amount of irrigation applied was measured with one in-line water meter placed at the beginning of the irrigation sector and connected to the telemetry system to detect any flow rate failure. It should be noted that irrigation events could occur at any time of the day.

Irrigation was managed according to $\theta_{v\text{-}soil}$ threshold values based on the concept of Management Allowed Deficit (MAD) [37] as the maximum average root zone stress at which optimum crop production will occur. Then, we adapted to the following equation.

$$MAD = \alpha/100 \times AWC$$

Where α is a percentage of the total available soil water content (AWC = the difference between FC – PWP ($m^3\ m^{-3}$).

Irrigation was automatically activated (trigger irrigation ON) when the mean $\theta_{v\text{-}soil}$ values in the 0–0.5 m soil profile (active root zone, [38]) reached the lower limit = FC – MAD. Meanwhile, irrigation OFF at FC (upper $\theta_{v\text{-}soil}$ threshold value).

The following irrigation criteria were applied:

(i) Moderate soil water deficit (α = 50 %, corresponds to a lower limit $\theta_{v\text{-}soil} = 0.215\ m^3\ m^{-3}$), from DOY 181 to 210.
(ii) Severe soil water deficit (α = 100 %), irrigation was withheld from DOY 211 to 245
(iii) Recovery: Irrigation recovered with full crop water requirements (100 % ETc) when $\Psi_{s,md}$ reached −2.0 MPa, from DOY 246 to 280.

The radio transmission units sent data to a gateway which was connected to an addVANTAGE web server (ADCON Telemetry, Vienna, Austria) for data processing and visualisation.

Measurements

Discrete determinations of $\Psi_{s,md}$, and leaf gas exchange parameters were made weekly on clear days to estimate the plant water status.

$\Psi_{s,md}$ was measured using a pressure chamber (Soil Moisture Equip. Crop. Model 3000, Santa Barbara, CA, USA), on mature leaves located on the shaded side of the tree and near the tree trunk at 13:00–14:00 h, GMT+2. Leaves were covered with foil ziplock bags for at least 2 h before the measurements [20]. One leaf per tree was cut from one replicate of each treatment and immediately placed in the chamber following the recommendations of [20].

Stomatal conductance (g_s mmol $m^{-2}\ s^{-1}$) was measured in one mature sunny leaf per tree in each replicate ($n = 4$) in the early morning (9:00–10:00 h, GMT+2), using a portable gas exchange system (LI-COR, LI-6400) at a photon flux density (PPFD) ≈ 1500 μmol$m^{-2}\ s^{-1}$ and CO_2 concentration ≈ 400 μmol mol^{-1}.

Moreover, daily courses of both indicators of plant water status were conducted at the end of periods of moderate deficit (α = 50 %, 29th July 2022, DOY 210), severe deficit (α = 100 %, 1st September 2022, DOY 244) and recovery (well-irrigated, 7th October 2022, DOY 280). On these dates, $\Psi_{s,md}$ and g_s were measured hourly on one leaf per tree in each replicate ($n = 4$). Leaf water potential (Ψ_{pd}, MPa), from uncovered leaves, was obtained on each daily course at predawn (05:30–06:30 h, GMT+2).

Dielectric permittivity (K), apparent electrical conductivity (EC_{bulk}), and trunk temperature (T_{trunk}) were continuously monitored with TDR-305 N (Acclima Inc., Meridian, USA) sensors. The sensor consists of three 0.05 m long waveguides, with all the electronics required for pulse generation and waveform acquisition embedded in a miniaturised circuit inside the probe, and the processed data transmitted via SDI-12 protocol. TDR-305 N sensors were embedded directly into the trunk located on the north-shaded side of the nectarine trees, in three out of the four replicates ($n = 3$), using a waveguide insertion tube with three parallel holes of 7 mm diameter. The holes were drilled in the required position (vertical in our case), diameter and depth for a perfect fit (Illustration 1). When installing the sensor, the manufacturer's recommendations described in Schwartz et al. [39] were considered. The sensor was the insulated with a thermal blanket following the recommendations of Saito et al. [40]. Data were collected every 15 min and transmitted using the same telemetry network used for $\theta_{v\text{-}soil}$.

Leaf osmotic potentials (Ψ_π) were determined on the same leaves used for Ψ_{pd} (*e.g.* at predawn (05:30–06:30 h GTM+2)), coinciding with daily time courses. Leaves were frozen in liquid nitrogen and osmotic potential was measured after thawing the samples and squeezing the sap using a vapour pressure osmometer (model WESCOR-5520; Wescor Inc., Logan, UT, USA) following the recommendations of Gucci et al. [41]. Leaf turgor potentials (Ψ_t) were calculated as the difference between osmotic and leaf water potentials. Leaf osmotic potential at full turgor ($\Psi_{\pi 100}$) was measured on leaves adjacent to those used for Ψ_{pd} at predawn. The leaves were excised and immediately their petioles placed in distilled water overnight to reach full saturation, after which they were frozen in liquid nitrogen (−196 °C), stored at −30 °C, and $\Psi_{\pi 100}$ measured after thawing the samples following the same methodology as for Ψ_π.

Calibration procedure

A representative healthy field-grown nectarine tree was selected for TDR-trunk calibration. First, the trunk was separated from the canopy and the main shoots using a power saw. A section of approximately 0.15 m (height) was excised and completely covered with a transparent film to prevent water losses and placed in a portable cool box (Illustration 2a). Then, the trunk sections were taken to the lab in an isolated box where the TDR-305 N sensor was installed, following the instructions described above, and the assembly was mounted on a digital weighing scale under ambient room conditions. The TDR-305 N sensor was connected to a laptop to continuously monitor K-data and trunk weight, until weight loss was constant (Illustration 2b). The procedure was repeated in three different trunk sections.

Statistical analysis

Data were depicted using the software SigmaPlot v. 14.5 (Inpixon, PA, USA). Statistical comparisons were considered significant at $p < 0.05$, using Pearson's correlation matrix. For K data, the hourly moving average (MA) was calculated to visualise trends and smooth noise obtained by the TDR-trunk sensors. Relationships between plant and soil water status indicators were explored by linear and quadratic regression analyses. The degree of agreement of the regressions between variables was assessed by the coefficient of determination (r^2) and the mean square error (MSE). All analyses were performed with SPSS v. 9.1 (IBM, Armonk, NY, USA).

Results and discussion

Soil water relations

During the experimental period, which included the postharvest period (DOY 180–280), the amount of water applied in the automated soil-based treatment amounted to 86 mm (Fig. 1a). This low dose is

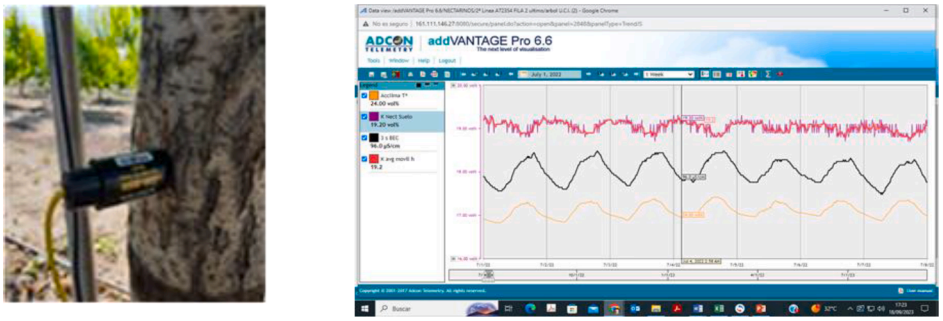

Illustration 1. Details of TDR-305 N installed on the field-nectarine tree trunk, and data visualisation (K, purple colour and it moving average, $K_{MA,}$ red colour), $EC_{bulk,}$ black colour and $T_{trunk,}$ orange colour) on the addVANTAGE web server.

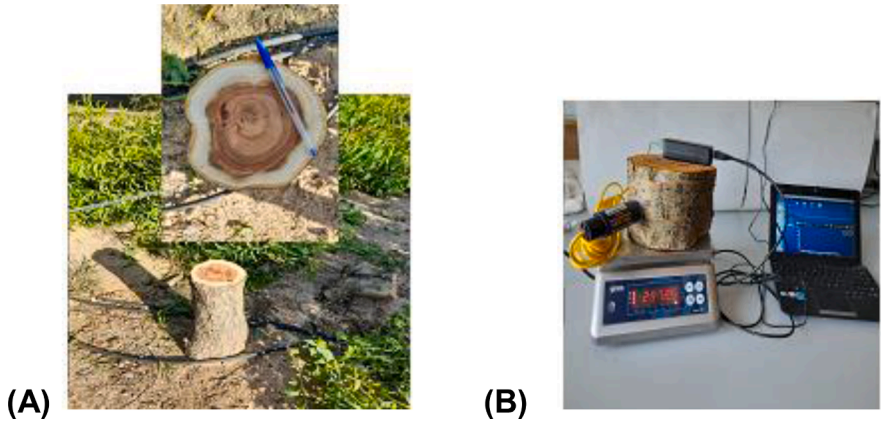

Illustration 2. (A) Excised nectarine tree trunk section in the field; (B) Monitoring K (TDR-305 N sensor) and trunk weight in the laboratory.

because the study includes a severe deficit period in which irrigation was withheld coinciding with the annual period of highest evaporative demand (August, DOY 211–245) (Fig. 1a). For the same experimental orchard, the regular water requirements during the postharvest period of well irrigated nectarine trees ranged from 427 to 572 mm [16,17].

In this field-experiment, a quite different postulate was applied, where the MAD concept was managed with capacitance probes to reach different irrigation conditions. Fig. 1b shows the mean $\theta_{v\text{-}soil}$ values of

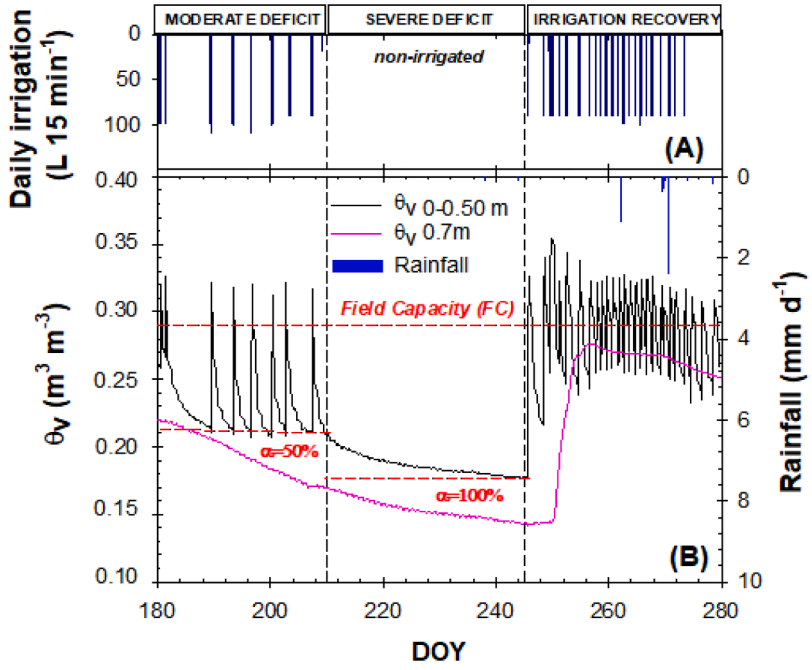

Fig. 1. Seasonal trend of: (A) daily irrigation events; and (B) average soil water content ($\theta_{v\text{-}soil}$, $m^3\ m^{-3}$) in the 0–0.50 m soil profile (black line), and at 0.70 m (pink line) along with daily rainfall events (vertical blue lines). Dashed horizontal red lines correspond to FC and soil irrigation condition: moderate deficit (DOY 180–210), severe deficit (DOY 211–245), and irrigation recovery (DOY 246–280), respectively. Dashed vertical black lines delimit each irrigation period. DOY: Day of the year.

the 0 − 0.50 m soil depths, which corresponded to the area of maximum root density of *Prunus* trees, as indicated in a previous experiment within the orchard [38], together with the 0.7 m profile to determine water losses by leaching. In the period of moderate soil water deficit (α = 50 %), irrigation was triggered when the $\theta_{v\text{-}soil}$ threshold value of 0.215 m^3 m^{-3} was reached and stopped at field capacity (FC = 0.29 m^3 m^{-3}). This protocol induced an irrigation interval of 2 or 3 days. De la Rosa et al. [42] found $\theta_{v\text{-}soil}$ values (≈ 0.30 m^3 m^{-3}) in fully irrigated nectarine trees cultivated also in clay-loam soils. In the period of severe water deficit (no irrigation applied), α = 100 % caused a gradual decrease of $\theta_{v\text{-}soil}$ reaching a minimum value of MAD = 0.17 m^3 m^{-3} at the end of the period, close to the permanent wilting point value. Interestingly, the $\theta_{v\text{-}soil}$ at 0.7 m denoted full water extraction by plant roots reaching a minimum value of 0.15 m^3 m^{-3} just before irrigation recovery started. This fact showed that there is also an effective water extraction in the deeper soil profiles during the process of soil drying. Periods of severe drying significantly modify the conditions of hydrologic flow path and impair their water retention capabilities [43]. Likewise, during the recovery period when irrigation was restored to meet full crop water requirements, $\theta_{v\text{-}soil}$ varied around FC values, ranging between 27−32 % in response to irrigation and, to a lesser extent, to rainfall events (Fig. 1a, b). As plant roots absorb water and the soil dries, $\theta_{v\text{-}soil}$ fluctuations depend not only on irrigation or rainfall events, but also on root water uptake dynamics and diurnal environmental changes [44]. Mira-García et al. [18] confirmed in a pot experiment that $\theta_{v\text{-}soil}$ variations were closely related to evapotranspiration demand, revealing the sensitivity of capacitance sensors to the nearby environment of soil, plant roots and atmosphere.

Plant water relations

The water relations of the plants evaluated in the experiment reflected the MAD-based irrigation protocol (Fig. 1b) as well as the climatic conditions (Fig. 2a). Examining the 10-year seasonal average values of ET_0 and rainfall (≈ 1320 and 250 mm, respectively), the climatic conditions recorded during the experimental postharvest period were consistent with the characteristics of the semi-arid Mediterranean environment [45], with ET_0 values amounting to 490.5 mm and low rainfall (10.4 mm, Fig. 1B). Daily ET_0 was highest (4.77 mm) in July (DOY 204) and lowest (0.73 mm) in September (DOY 258). A similar pattern was observed in VPD values but with high day-to-day variability. Noguera et al. [46] recently reported that VPD variability seems to be less coupled with soil moisture variability during summer, while it is better correlated during winter. VPD variability would be mainly related to climate variability mechanisms controlling temperature and relative humidity rather than to feedback in the soil-plant-atmosphere continuum [24].

The seasonal dynamics of midday stem water potential ($\Psi_{s,md}$) and leaf stomatal conductance (g_s) are represented in Fig. 2b. Initially, plant indicator values corresponded to nectarine trees subjected to any irrigation water limitation ($\Psi_{s,md}$ = −0.72±0.01, and g_s = 225±12.8) ([15, 42,47], 2021). As soon as deficit irrigation of the soil was initiated, $\Psi_{s,md}$ and g_s started to decrease, registering their lowest values at the end of the severe water deficit period (DOY 237) ($\Psi_{s,md}$ = −2.05±0.06 and g_s= 63.5 ± 9.05). Despite irrigation recovery, g_s values were slightly lower than those observed at the beginning of the study due to leaf senescence [48]. Partial defoliation has been shown to affect water relations and plant gas exchange [49]. The lower values in gas exchange in the late postharvest period by a decrease in the amino acid aspartate affecting chloroplast formation in nectarine leaves [24].

Dielectric permittivity (K) and bulk electrical conductivity (EC_{bulk}) values showed a similar pattern to that introduced in the MAD irrigation soil water content (Fig. 3b,c). K & EC_{bulk} varied with soil water deficit, with average values of 18.62±0.07 & 86.83±1.99 μS cm^{-1}, 17.59±0.06 & 62.26±0.55 μS cm^{-1}, and 17.85±0.06 & 72.44±0.78 μS cm^{-1}in the moderate and severe deficits, and irrigation recovery periods,

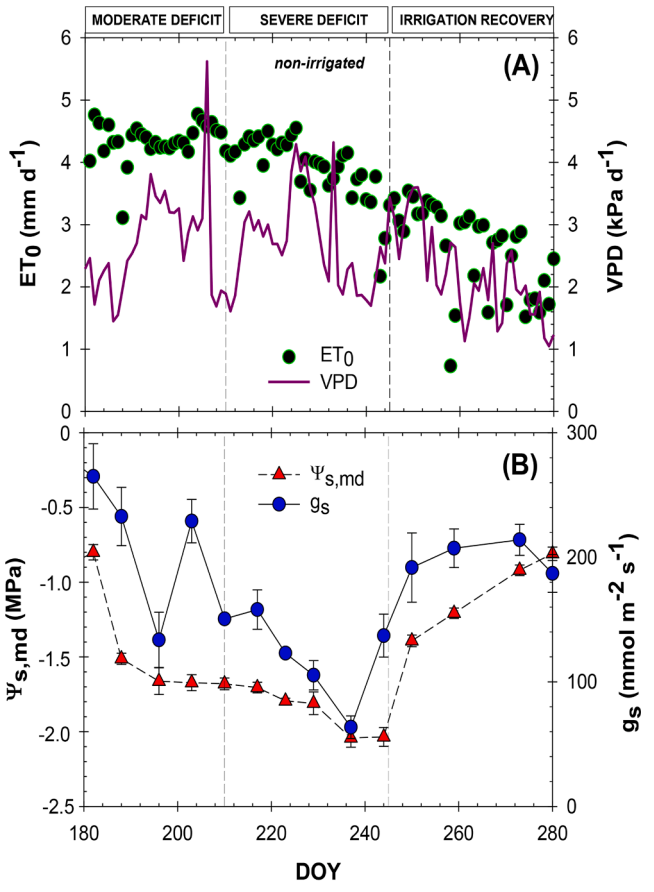

Fig. 2. Seasonal trend of: (A) daily evapotranspiration (ET_0, mm) and vapour pressure deficit (VPD, kPa); and (B) midday stem water potential ($\Psi_{s,md}$, MPa) and stomatal conductance (g_s, mmol m^{-2} s^{-1}). Each point is the average of four leaves ± ES. Dashed vertical black lines delimit each irrigation period. DOY: Day of the year.

respectively. As expected, the lowest values of K and EC_{bulk} were observed in the severe deficit period, and the highest during the irrigation recovery period. However, the difference between both irrigation periods were not too much high. This may be attributed to either lower xylem conductivity or to lower canopy transpiration, both caused by partial defoliation typical of the late postharvest period [49]. In this regard, a strong curve-linear relationship was observed between K and EC_{bulk} (R^2=0.92, $p < 0.001$) (Fig. 4).

Although K represented well the MAD-based irrigation protocol, in the experimental conditions its values fluctuated in a very short range (only 2 units). This result could be explained by the 5 cm length of the TDR-rods that detect the inner part of the xylem of the less conductive vessels [26]. However, EC_{bulk} offers a wider range (approximately 60 units). The seasonal trend in trunk temperature (T_{trunk}) (Fig. 3a) was more dependent on weather conditions (Fig. 2a) than on $\theta_{v\text{-}soil}$ variations (Fig. 1). Similarly, in a study with oaks, Hernández-Santana et al. [50] observed comparatively less variation in stem water content (14 %) compared to measurements of soil water content or water+ potential (averaging 50 %). This finding is noteworthy given that stem water content showed the greatest sensitivity to reductions in soil water content.

Plant water relations in daily time courses were assessed on representative days at the end of periods of moderate water deficit (DOY 210), severe water deficit (DOY 245), and irrigation recovery (DOY 280). In Fig. 5, diurnal patterns of $\Psi_{s,md}$ and g_s are plotted together with VPD and global radiation. The diurnal patterns of plant water relations comprised the imposed soil water deficit, despite the different prevailing climatic

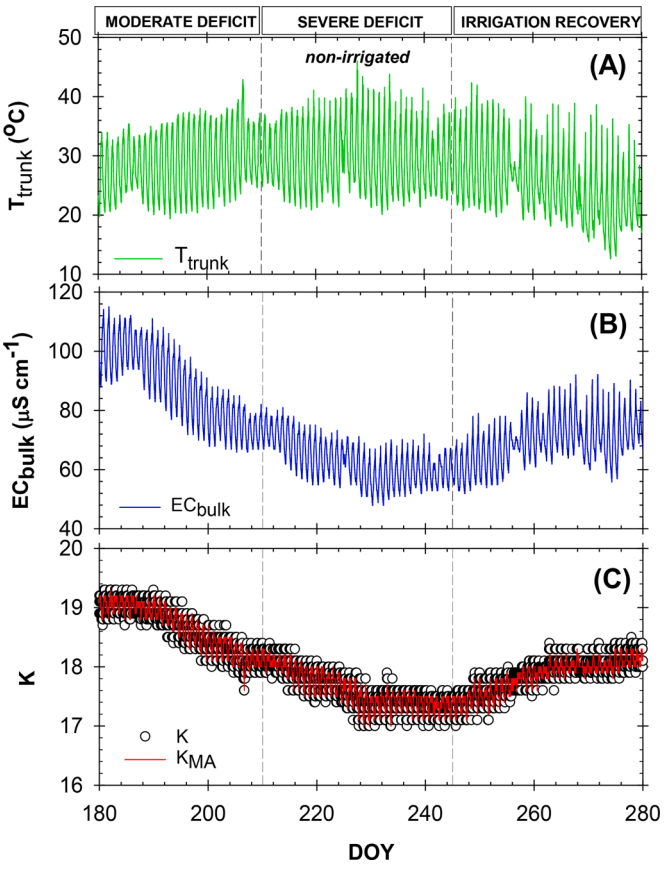

Fig. 3. Seasonal values at 15 min recorded with a trunk-TDR-305N: (A) temperature (T_{trunk}, °C); (B) bulk electrical conductivity (EC_{bulk}, µS cm^{-1}); and (C) relative dielectric permittivity (K) and the hourly moving average K (K_{MA}, red line) during the experimental period. Values are averages of three TDR sensors. The vertical dashed lines delimit each irrigation period. DOY: Day of the year.

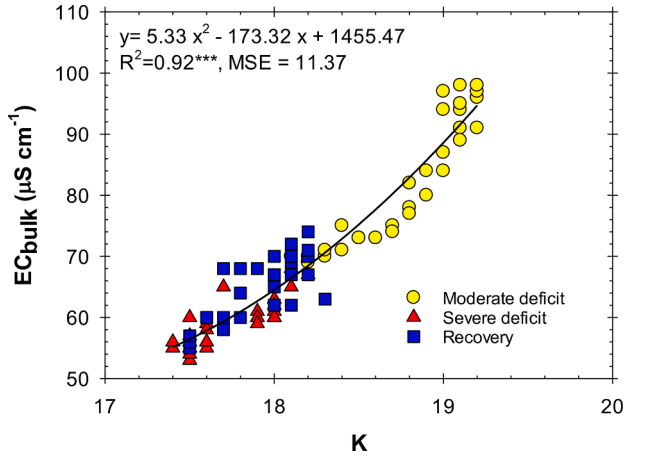

Fig. 4. Relationship between dielectric permittivity (K) and bulk electrical conductivity (EC_{bulk}) monitored with trunk-TDR-305 N. Values correspond to daily averages of three TDR sensors, at each irrigation period: moderate deficit or α = 50 % (yellow circle); severe deficit or α = 100 % (red triangles); and recovery irrigation or well-irrigated (blue squares). ***; $p \leq 0.001$.

conditions recorded (Fig. 5a–c). In this sense, the most demanding day was observed in the period of severe water deficit (1st September, DOY 245), and the lowest in the period of irrigation recovery (7th October, DOY 280).

During the three diurnal courses, the lowest values of $\Psi_{s,md}$ were observed in the early afternoon (16:00 h GTM+2), averaging −1.76 ± 0.03 MPa (moderate water deficit), −1.89 ± 0.03 MPa (severe water deficit), and −0.95 ± 0.04 MPa (irrigation recovery), respectively. In line with this, the values of Ψ_{pd} followed the same trend of $\Psi_{s,md}$, varying from −0.68 ± 0.03 and −0.81 ± 0.11 MPa in the moderate and severe deficit periods to −0.40 ± 0.05 in the irrigation recovery period (Fig. 5D-f, Table 1), respectively. Moreover, they coincided with those reported by Girona et al. [51] in deficit irrigated peach trees. Since they are taken at night, when there is no transpiration, the Ψ_{pd} values indicate the water status of the soil surrounding the roots [52]. However, if there are large variations in soil water content within the profile, inaccurate values may occur [53].

For its part, g_s has been observed to affect the rate of assimilation [54]. The observed circadian pattern for g_s was characterised by maximal stomatal opening from sunrise, as soon as radiation reached the plant leaves, at 08:00 until 10:30 h GTM+2, followed by a decreasing trend with minimal values reached by midday. A slight increase in g_s was also observed during the afternoon hours, which may be a consequence of easing environmental conditions [55].

The daily time-courses of T_{trunk}, EC_{bulk} and K are shown in Fig. 6. K & EC_{bulk} values fluctuated in a range of 17.2 − 18.3 & 67−81 µS cm^{-1}, 17.1 − 17.5 & 53−67 µS cm^{-1}, and 18.0 − 18.3 & 63−89 µS cm^{-1} at moderate and severe deficits, and irrigation recovery periods, respectively (Fig. 6b). T_{trunk} values increased around midday and recorded the lower absolute values during irrigation recovery, as this was the least demanding day (Fig. 2a). The fact that K decreases during the day and increases at night proves that the sensors are able to detect diurnal fluctuations in tree trunk hydration [30,31]. Moreover, the soil water deficit reduced the values of K (Fig. 6H). Thus, the intensity of the response of the stem water content is related to the intensity of the soil water deficit ([27]a).

EC_{bulk} behaved in the same pattern as T_{trunk}, suggesting that an increase in temperature results in higher ion mobility in the wood sap, leading to an increase in EC_{bulk} [56].

An interesting work by Stott et al. [57] compared four commercially available sensors (GS3 from Meter Group, Inc., Pullman, WA, USA, CS655 from Cambpell Scientific, Inc., Logan, UT, USA, and TDR-315/315 L from Acclima, Inc., Boise, ID, USA). The study concluded that changes in the T_{trunk} also affect the EC_{bulk}, so caution should be taken with temperature sensitivity, even if the sensor has been previously insulated [40]. However, the authors suggested that diurnal changes in trunk hydration, although interesting, may be less valuable for irrigation scheduling based on water content in the trunk ($\Theta_{v\text{-}trunk}$) than daily averages, especially when there is doubt about the effect of temperature on the measurements.

As expected, soil water deficit lowered leaf water potential (Ψ_{pd}) and actual osmotic potential (Ψ_o) (Table 1). No significant differences in osmotic water potential were observed at full turgor ($\Psi_{\pi 100}$) and even in the irrigation recovery period, leaf turgor potential (Ψ_t) decreased as the season progressed due to leaf senescence [49]. Accelerated leaf senescence and leaf abscission can occur, which is associated with episodes of drought (in our case, severe water deficit period), meaning that canopy size decreases due to turgor loss [58]. Lower values of EC_{bulk} measured with trunk-TDR-315 N were associated with higher (less negative) values of Ψ_o, under well-irrigated conditions, probably due to a lower amount of osmolytes through a dilution effect [59]. No osmotic adjustment was observed in the experiment. In this sense, Mellisho et al. [60] in peach trees and Ruiz-Sánchez et al. [61] in apricot trees reported that a $\Psi_{s,md.}$ value below –2.0 MPa must be achieved over a long period of time to activate this tolerance mechanism.

Fig. 7 shows a strong dependency between the irrigation protocol based on threshold $\theta_{v\text{-}trunk}$ values with plant water status, both stem water potential ($\Psi_{s,md}$) and trunk permittivity (K), with the changes in $\Psi_{s,md}$ and K over 75 % by $\theta_{v\text{-}trunk}$ variations. Soil water content is an indicator of the availability of water for plant consumption [1]. These results confirm that plants perceive a water deficit in the soil and that

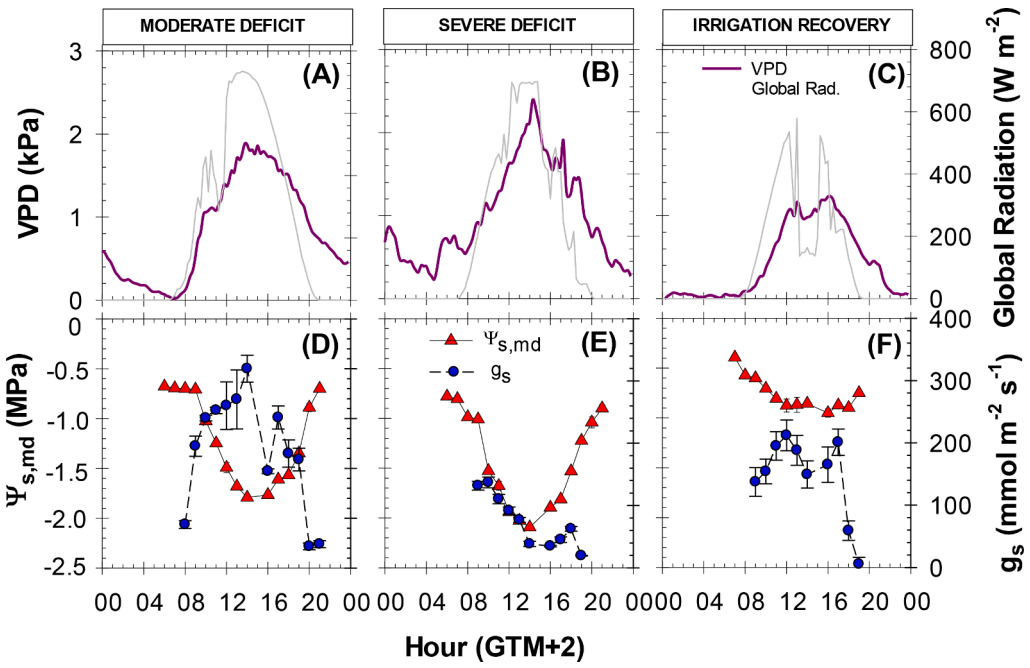

Fig. 5. Daily values of: (A) vapour pressure deficit (VPD, kPa) and global radiation (W m^{-2}); and (B) midday stem water potential ($\Psi_{s,md}$, MPa) and stomatal conductance (g_s, mmol m^{-2} s^{-1}) at the end of each irrigation period: α = 50 %, moderate deficit (DOY 210); α = 100 %, severe deficit (DOY 245); recovery irrigation, well irrigated (DOY 280). Each point is the average of four leaves ± ES. DOY: Day of the year.

Table 1
Values of predawn leaf water potential (Ψ_{pd}, MPa); osmotic actual potential (Ψ_o, MPa), osmotic potential at full turgor ($\Psi_{\pi 100}$, MPa); and leaf turgor potential (Ψ_t, MPa) at the end of each irrigation period: moderate deficit (α = 50 %, DOY 210); severe deficit (DOY 245, α = 100 %,); and irrigation recovery (DOY 280, well-irrigated).

Irrigation period	Ψ_{pd}	Ψ_o	$\Psi_{\pi 100}$	Ψ_t
Moderate deficit	−0.68	−2.23	−1.80	1.55
	±0.01b	±0.01b	±0.02	±0.01b
Severe deficit	−0.81	−2.52	−1.77	1.71
	±0.04c	±0.03c	±0.05	±0.04a
Irrigation	−0.40	−1.61	−1.72	1.26
recovery	±0.02a	±0.02a	±0.04	±0.02c
Average	−0.63	−2.12	−1.76	1.5
ANOVA	***	***	n.s.	***

ANOVA: Analysis of variance***: $p < 0.01$. n.s.: not significant.

this information is important for precise irrigation scheduling [21]. It is known that the factors that affect K are temperature, soil moisture and frequency [5,29]. The loss of K at higher $\theta_{v\text{-}trunk}$ values coinciding with irrigation recovery and less demanding weather conditions (Fig. 2a) is quite striking (Fig. 7b). This fact is probably due to a loss of xylem conductivity corresponding to the phenological period of late post-harvest. In this sense, Sparks et al. [33] reported that losses in stem hydraulic conductivity correlated with freeze-thaw events during warming periods in midwinter that reduced stem water content.

Conversion of K into $\theta_{V\text{-}trunk}$

As the trunk water content is a recognised water status indicator, the conversion of K TDR-values into $\Theta_{V\text{-}trunk}$ values was performed. For this purpose, the results of the calibration, which was performed according to the procedure described in the methodology section, are shown in Fig. 8. At the end of the drying period, when the weight loss was constant (46 days), K reached a value of 6.7. Therefore, weight loss of 30 % corresponded to a K loss of 11 units (Fig. 8a). Correlation of the calibration data showed a perfect quadratic fit (Fig. 8b). However, since we moved in a short range of K values (17.0–19.4), we applied the least squares method, which determines the linear regression line that minimises the residuals [62]. Then, using the equation obtained in Fig. 8c, the K values were converted to $\theta_{v\text{-}trunk}$.

The trend of the two plant indicators was very similar (Fig. 9). Only at the beginning of the study (moderate deficit) were the daily values of K slightly higher than those of the $\theta_{v\text{-}trunk}$, but this effect was not significant. Therefore, TDR-305 N sensor was well suited for measuring water content in the nectarine trunk and could be properly used for monitoring daily and seasonal changes in K.

Conclusions

Novel trunk-TDR sensors embedded directly in the tree trunk were able to reveal automated $\theta_{v\text{-}soil}$-based irrigation protocols applied in a nectarine tree orchard. Continuous K measurements explained more than 75 % of $\theta_{v\text{-}soil}$ variation as in the case of $\Psi_{s,md}$. Furthermore, the calibration of K measurements into $\theta_{v\text{-}trunk}$ values proposed in this study could be extended to other fruit crops.

The different behaviour of K and EC_{bulk} on a daily and seasonal scale was due to dilution effects of the ions due to higher sap flow and transpiration during the day as well as water content and its movement in the soil during the season. In addition, the results showed the impact of leaf senescence during the late postharvest period, when irrigation resumed, on the K response, so additional information is needed early in the season to verify K threshold values under non-limiting soil water conditions.

Since automation is possible with real-time K data (or $\theta_{v\text{-}trunk}$ instead), further research is needed to determine threshold K values for successful precision irrigation. In addition, the stability and long-term performance of trunk-TDR sensors need to be verified.

This work showed promising findings on the use of trunk water content sensors for accurate continuous monitoring of the plant water status of nectarine trees.

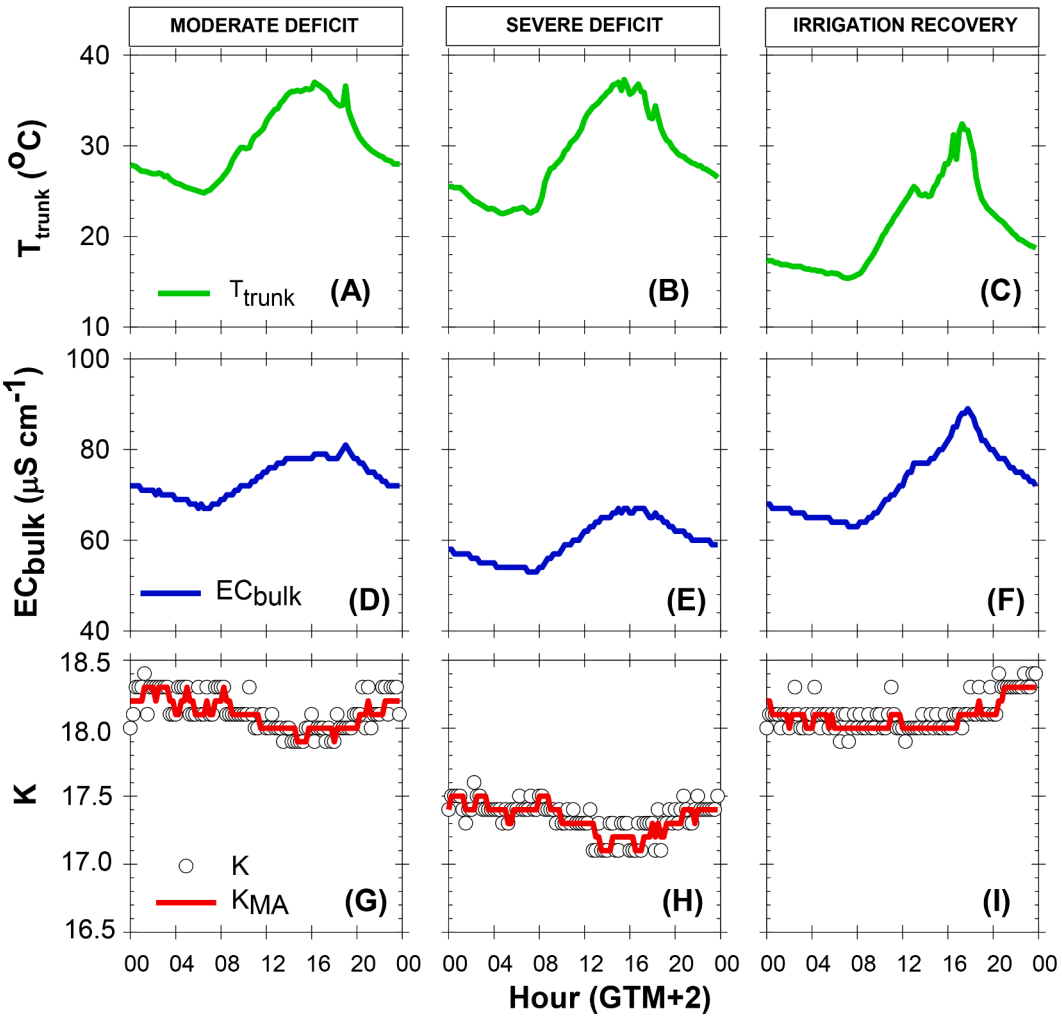

Fig. 6. Daily patters of (A-C) trunk temperature (T_{trunk}), (D-F) bulk electrical conductivity (EC_{bulk}), and (G-I) relative dielectric permittivity (K) and their 15 min-moving average (K_{MA}) recorded with trunk-TDR-305 N. The values shown corresponded to those at the end of each irrigation period: α = 50 %, moderate deficit (DOY 210); α = 100 %, severe deficit (DOY 245); recovery irrigation, well-irrigated (DOY 280). The values are means of three TDR sensors. DOY: Day of the year.

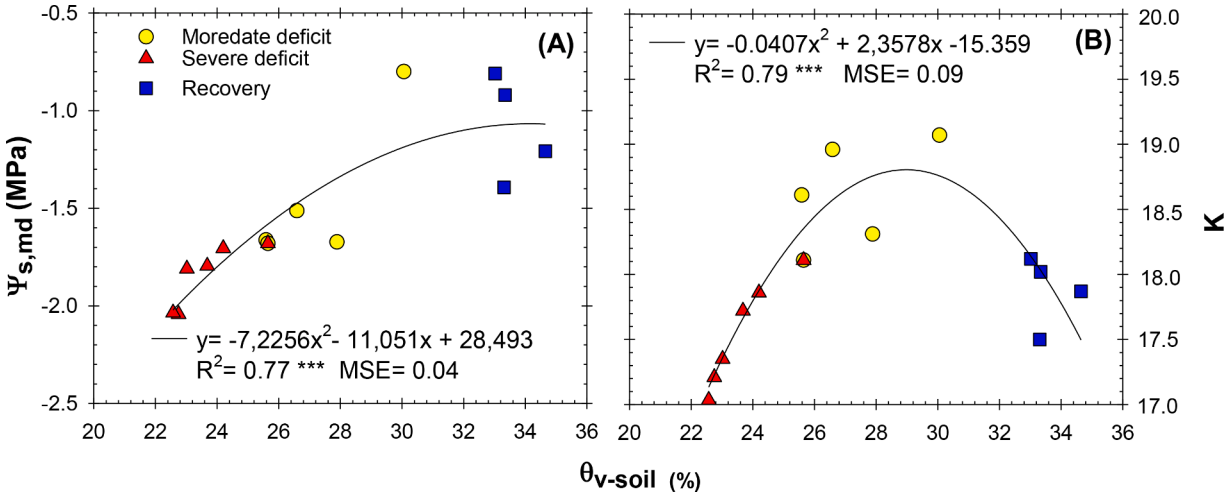

Fig. 7. Relationship between soil water content in the 0–0.5 m soil profile ($\theta_{v\ 0-50cm,\ \%}$) *vs./and*: (A) stem water potential at midday ($\Psi_{s,md}$, MPa); and (B) dielectric permittivity (K) monitored with trunk-TDR-305 N. The average daily values of $\Theta_{v\text{-}soil}$ and K coincided with the days on which $\Psi_{s,md}$ values were determined during each irrigation period: moderate deficit or α = 50 %, (yellow circle); severe deficit or α = 100 %, (red triangles); and recovery irrigation or well-irrigated (blue squares). Values are means of four capacitance probes and leaves and three TDR sensors. ***, $p \leq 0.001$.

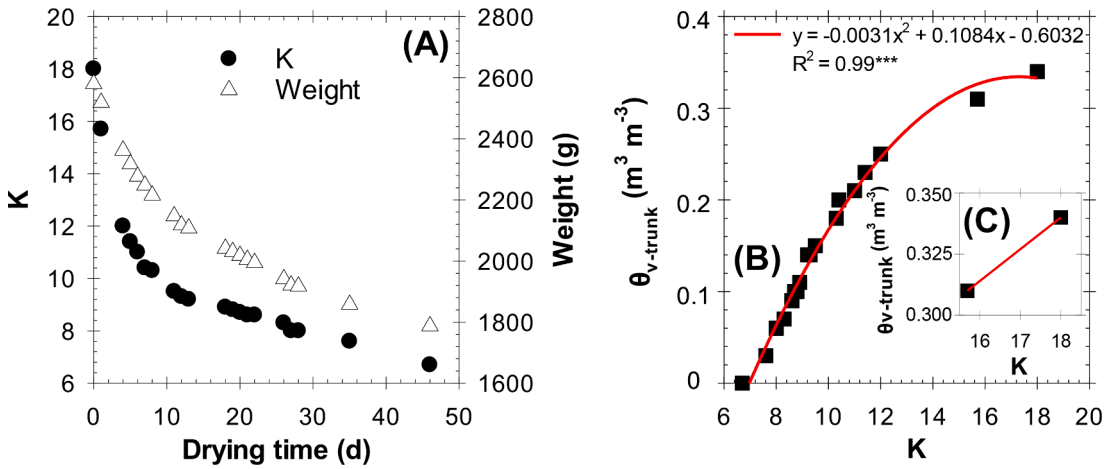

Fig. 8. (A) Dynamic of K and trunk weight during the drying time; and (B, C) relationship between K and $\theta_{v\text{-trunk}}$. In (C) the equation is: $y = 0.013\ x + 0.1052$; r^2=0.99***. Values are mean of three replicates.

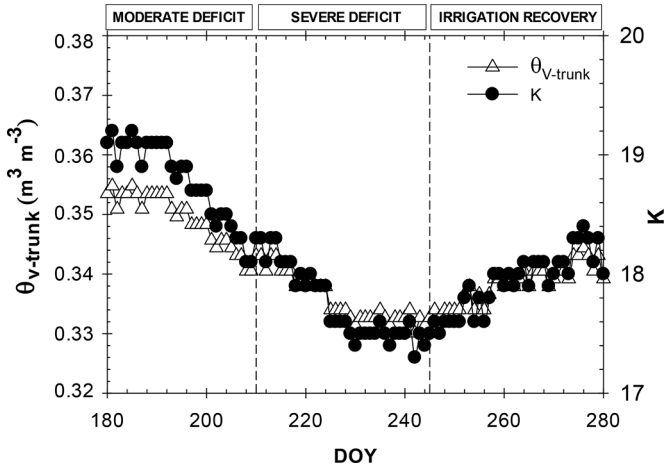

Fig. 9. Seasonal values of dielectric permittivity (K) and estimated trunk water content ($\theta_{v\text{-trunk}}$, $m^3\ m^{-3}$) monitored by trunk-TDR-305 N sensors.

CRediT authorship contribution statement

María R. Conesa: Conceptualization, Data curation, Formal analysis, Investigation, Resources, Supervision, Validation, Visualization, Writing – original draft, Writing – review & editing. **Juan Vera:** Conceptualization, Investigation, Methodology, Resources, Software, Validation, Writing – review & editing. **Wenceslao Conejero:** Conceptualization, Data curation, Formal analysis, Investigation, Methodology, Resources, Validation, Visualization, Writing – review & editing. **Virginia Hernandez-Santana:** Resources, Validation, Writing – review & editing. **María Carmen Ruiz-Sánchez:** Conceptualization, Funding acquisition, Investigation, Project administration, Supervision, Writing – review & editing, Resources, Validation.

Declaration of competing interest

The authors declare that they have no known competing financial interests or personal relationships that could have appeared to influence the work reported in this paper.

Data availability

Data will be made available on request.

Acknowledgments

This work was funding by the project from the Spanish State Agency PID2019-106226RB-C21/AEI/10.13039/501100011033 and AGROALNEXT (PRTR-C17.I1) supported by MCIN with funding from European Union NextGenerationEU (PRTR-C17.I1) and by Fundación Séneca with funding from Comunidad Autónoma Región de Murcia (CARM). M. R. Conesa thanks to the Spanish JdlC programme (IJC2020-045450-I) funded by MCIN/AEI/10.13039/501100011033 and European Union NextGenerationEU/PRTR.

References

[1] N. Katerji, M. Mastrorilli, G. Rana, Water use efficiency of crops cultivated in the Mediterranean regions: review and analysis, Europ. J. Agron. 28 (4) (2008) 493–507, https://doi.org/10.1016/j.eja.2007.12.003.
[2] I. Fernández-García, S. Lecina, M.C. Ruiz-Sánchez, J. Vera, W. Conejero, M. R. Conesa, A. Domínguez, J.J. Pardo, B.C. Llélis, P. Montesinos, Trends and challenges in irrigation scheduling in the semi-arid area of Spain, Water. (Basel) 12 (2020) 785, https://doi.org/10.3390/w12030785.
[3] E. Vories, K. Sudduth, Determining sensor-based field capacity for irrigation scheduling, Agric. Water Manage. 250 (2021) 106860, https://doi.org/10.1016/j.agwat.2021.106860.
[4] P. Charlesworth, Soil Water Monitoring (Irrigation Insights n°. 1, 2ndEd.), Australia: CSIRO Land and Water, 2005, p. 96, pp.
[5] J. Vera, W. Conejero, A.B. Mira-García, M.R. Conesa, M.C. Ruiz-Sánchez, Towards irrigation automation based on dielectric soil sensors, J. Hort. Sci. Biotech. 96 (6) (2021) 696–707, https://doi.org/10.1080/14620316.2021.1906761.
[6] J.M. Domínguez-Niño, J. Casadesús, H.R. Bogena, J.A. Huisman, Reliability of capacitance type soil moisture sensors for their use in automated scheduling of drip irrigation in orchards, Acta Hortic. 1335 (2022) 381–388, https://doi.org/10.17660/ActaHortic.2022.1335.47.
[7] M.R. Conesa, W. Conejero, J. Vera, J.M. Ramírez-Cuesta, M.C. Ruiz-Sánchez, Terrestrial and remote indexes to assess moderate deficit irrigation in early-maturing nectarine trees, Agronomy 9 (10) (2019) 630, https://doi.org/10.3390/agronomy9100630.
[8] R.G. Allen, J.S. Pereira, D. Raes, M. Smith, Crop evapotranspiration: Guidelines for Computing Crop Water Requirements, 56, FAO, Rome (Italy), 1998, p. 300.
[9] S. Millán, J. Casadesús, C. Campillo, M.J. Moñino, M.H. Prieto, Using soil moisture sensors for automated irrigation scheduling in a plum crop, Water (Basel) 11 (2019) e2061, https://doi.org/10.3390/w11102061.
[10] J.M. Domínguez-Niño, J. Oliver-Manera, G. Arbat, J. Girona, J. Casadesús, Analysis of the variability in soil moisture measurements by capacitance sensors in a drip-irrigated orchard, Sensors 20 (18) (2020) 5100, https://doi.org/10.3390/s20185100.
[11] S.R. Evett, Soil water and monitoring technology (Ed.), in: R.J. Lascano, R.E. Sojka (Eds.), Irrigation of Agricultural Crops, 2nd ed, Agron. Monogr, ASA, CSSA, and SSSA, Madison, WI, 2007, pp. 25–84, 30.
[12] S.R. Evett, K.C. Stone, R.C. Schwartz, S.A. O'Shaughnessy, P.D. Colaizzi, S. K. Anderson, D.J Anderson, Resolving discrepancies between laboratory-determined field-capacity values and field water content observations: implications for irrigation management, Irrig. Sci. 37 (2019) 751–759, https://doi.org/10.1007/s00271-019-00644-4.

[13] M.C. Ruiz-Sánchez, R. Domingo, J.R. Castel, Review. Deficit irrigation in fruit trees and vines in Spain, Span. J. Agric. Res. 8 (S2) (2010) 5–20, https://doi.org/10.5424/sjar/201008s2-1343.

[14] J. Vera, W. Conejero, M.R. Conesa, M.C. Ruiz-Sánchez, Irrigation factor approach based on soil water content: a nectarine orchard case study, Water. (Basel) 11 (2019) 589, https://doi.org/10.3390/w11030589.

[15] M.R. Conesa, W. Conejero, J. Vera, M.C. Ruiz-Sánchez, Effects of postharvest water deficits on the physiological behaviour of early-maturing nectarine trees, Plants 9 (2020) 1104, https://doi.org/10.3390/plants9091104.

[16] M.R. Conesa, W. Conejero, J. Vera, M.C. Ruiz-Sánchez, Soil-based automated irrigation for a nectarine orchard in two water availability scenarios, Irrig. Sci. 39 (2021) 421–439, https://doi.org/10.1007/s00271-021-00736-0.

[17] M.R. Conesa, W. Conejero, J. Vera, V. Agulló, C. García-Viguera, M.C. Ruiz-Sánchez, Irrigation management practices in nectarine fruit quality at harvest and after cold storage, Agric. Water Manage 243 (2021) 106519, https://doi.org/10.1016/j.agwat.2020.106519.

[18] A.B. Mira-García, J. Vera, W. Conejero, M.R. Conesa, M.C Ruiz-Sanchez, Evapotranspiration in young lime trees with automated irrigation, Sci. Hortic. 288 (2021) 110396, https://doi.org/10.1016/j.scienta.2021.110396.

[19] A.B. Mira-García, W. Conejero, J. Vera, M.C. Ruiz-Sánchez, Water status and thermal response of lime trees to irrigation and shade screen, Agric. Water Manage 272 (2022) 107843, https://doi.org/10.1016/j.agwat.2022.107843.

[20] H. McCutchan, K.A. Shackel, Stem water potential as a sensitive indicator of water stress in prune trees (*Prunus domestica* L. cv. French), J. Am. Soc. Hort. Sci. 4 (177) (1992) 607–611, https://doi.org/10.21273/jashs.117.4.607.

[21] H.G. Jones, Irrigation scheduling: advantages and pitfalls of plant-based methods, J. Exp. Bot. 55 (2004) 2427–2436, https://doi.org/10.1093/jxb/erh213.

[22] O. García-Tejera, A. López-Bernal, F. Orgaz, L. Testi, F.J. Villalobos, The pitfalls of water potential for irrigation scheduling, Agric. Water Manage. 243 (2021) 106522, https://doi.org/10.1016/j.agwat.2020.106522.

[23] P.F. Scholander, E.D. Bradstreet, E.A. Hemmingsen, H.T. Hammel, Sap pressure in vascular plants: negative hydrostatic pressure can be measured in plants, Science (1979) 148 (3668) (1965) 339–346, https://doi.org/10.1126/science.148.3668.339.

[24] M.R. Conesa, W. Conejero, J. Vera, M.C. Ruiz-Sánchez, Assessment of trunk microtensiometer as a novel biosensor to continuously monitor plant water status in nectarine trees, Front. Plant Sci. 14 (2023) 1123045, https://doi.org/10.3389/fpls.2023.1123045.

[25] P. Cruiziat, H. Cochard, T. Ameglio, Hydraulic architecture of trees: main concepts and results, Ann. Sci. For. 59 (2002) 723–752, https://doi.org/10.1051/forest:2002060.

[26] H. He, N.C. Turner, K. Aogu, M. Dyck, H. Feng, B. Si, J. Wang, J Lv, Time and frequency domain reflectometry for the measurement of tree stem water content: a review, evaluation, and future perspectives, Agric. For. Meteorol. 306 (2021) 108442, https://doi.org/10.1016/j.agrformet.2021.108442.

[27] V. Hernandez-Santana, J. Martínez-Fernández, C. Moran, Estimation of tree water stress from stem and soil water monitoring with time-domain reflectometry in two small forested basins in Spain, Hydrol. Process. 22 (2008) 2493–2501, https://doi.org/10.1002/hyp.6845.

[28] J.L. Davies, Relative permittivity measurements of a sand and clay soil *in situ*, Geol. Surv. Can., Ottawa, Pap 75-1C (1975) 361–365.

[29] G.C. Topp, J.L. Davis, A.P. Annan, Electromagnetic determination of soil-water content: measurement in coaxial transmission lines, Water Resour. Res. 16 (1980) 574–582, https://doi.org/10.1029/WR016i003p00574.

[30] A. Nadler, E. Raveh, U. Yermiyahu, S.R. Green, evaluation of TDR use to monitor water content in stem of lemon trees and soil and their response to water stress, Soil Sci. Soc. Am. J. 67 (2003) 437–448, https://doi.org/10.2136/sssaj2003.4370.

[31] A. Nadler, E. Raveh, U. Yermiyahu, S. Green, Stress induced water content variations in mango stem by time domain reflectometry, Soil Sci. Soc. Am. J. 70 (2006) 510–520, https://doi.org/10.2136/sssaj2005.0127.

[32] N.M. Holbrook, M. Burns, T. Sinclair, Frequency and time-domain dielectric measurements of stem water content in the arborescent palm, Sabal palmetto, J. Exp. Bot. 43 (1992) 111–119, https://doi.org/10.1093/jxb/43.1.111, 1992.

[33] J. Sparks, G. Campbell, A. Black, Water content, hydraulic conductivity, and ice formation in winter stems of Pinus contorta: a TDR case study, Oecologia 127 (2001) 468–475, https://doi.org/10.1007/s004420000587.

[34] H. Lambers, N.J. Barrow, P2O5, K2O, CaO, MgO, and basic cations: pervasive use of references to molecules that do not exist in soil, Plant Soil. 452 (2020) 1–4, https://doi.org/10.1007/s11104-020-04593-2.

[35] J. Vera, J.M. de la Peña, FERTIGA: Programa de Fertirrigación de Frutales, CEBAS-CSIC, Murcia, Spain, 1994, p. 69.

[36] S.R. Evett, J.A. Tolk, T.A. Howell, Soil profile water content determination, Vadose Zone J. 5 (2006) 894–907, https://doi.org/10.2136/vzj2005.0149.

[37] J.L. Merriam, A management control concept for determining the economical depth and frequency of irrigation, Trans. ASAE 9 (1966) 492–498, https://doi.org/10.13031/2013.40014.

[38] I. Abrisqueta, W. Conejero, L. López-Martínez, J. Vera, M.C. Ruiz-Sánchez, Root and aerial growth in early-maturing peach trees under two crop load treatments, Span. J. Agric. Res. 15 (2) (2017) e0803, https://doi.org/10.5424/sjar/2017152-10714.

[39] R.C. Schwartz, S.R. Evett, S. Anderson, D. Anderson, Evaluation of a direct-coupled TDR for determination of soil water content and bulk electrical conductivity, Vadose Zone J. 15 (1) (2016) 1–8, https://doi.org/10.2136/vzj20 15.08.0115.

[40] T. Saito, H. Yasuda, M. Sakurai, K. Acharya, S. Sueki, K. Inosako, K. Yoda, H. Fujimaki, M.A.M. Abd Elbasit, A.M. Eldoma, Monitoring of stem water content of native and invasive trees in arid environments using gs3 soil moisture sensors, Vadose Zone J. 15 (3) (2016) 1–9, https://doi.org/10.2136/vzj2015.04.0061.

[41] R. Gucci, C. Xiloyannis, J.A. Flores, Gas exchange parameters: water relations and carbohydrate partitioning in leaves of field-grown *Prunus domestica* following fruit removal, Physiol. Plant 83 (1991) 497–505, https://doi.org/10.1111/j.1399-3054.1991.tb00126.x.

[42] J.M. De la Rosa, R. Domingo, J. Gomez-Montiel, A. Pérez-Pastor, Implementing deficit irrigation scheduling through plant water stress indicators in early nectarine trees, Agric. Water Manage. 152 (2015) 207–216, https://doi.org/10.1016/j.agwat.2015.01.018.

[43] H. Zeng, C.S. Tang, Q. Cheng, C. Zhu, L.Y. Yin, B. Shi, Drought-induced soil desiccation cracking behaviour with consideration of basal friction and layer thickness, Water Resour. Res. 56 (7) (2020) e2019WR026948, https://doi.org/10.1029/2019WR026948.

[44] H. Li, J. Yi, J. Zhang, Y. Zhao, B. Si, R.L. Hill, L. Cui, X. Liu, Modeling of soil water and salt dynamics and its effects on root water uptake in Heihe arid Wetland, Gansu, China Water 7 (5) (2015) 2382–2401, https://doi.org/10.3390/w7052382.

[45] Eds. P. Lionello, F. Giorgi, E. Rohling, R. Seager, Chapter 3. Mediterranean climate: past, present and future, in: K. Schroeder, J. Chiggiato (Eds.), Oceanography of the Mediterranean Sea, Elsevier, 2023, pp. 41–91, https://doi.org/10.1016/B978-0-12-823692-5.00011-X. ISBN 9780128236925

[46] I. Noguera, S.M. Vicente-Serrano, D. Peña-Angulo, F. Dominguez-Castro, C. Juez, M. Tomás-Burguera, J. Lorenzo-Lacruz, C. Azorin-Molina, A. Halifa-Marin, B. Fernández-Duque, A. El Kenawy, Assessment of vapor pressure deficit variability and trends in Spain and possible connections with soil moisture, Atmos. Res. 285 (2023) 106666, https://doi.org/10.1016/j.atmosres.2023.106666.

[47] A. Naor, R. Stern, M. Peres, Y. Greenblat, Y. Gal, M.A. Flaishman, Timing and severity of postharvest water stress affect following year productivity and fruit quality of field-grown 'Snow Queen' nectarine, J. Amer. Soc. Hortic. Sci. 130 (2005) 806–812, https://doi.org/10.21273/JASHS.130.6.806.

[48] P.C. Andersen, B.V. Brodbeck, Water relations and net CO_2 assimilation of peach leaves of different ages, J. Am. Soc. Hortic. Sci. 113 (1988) 242–248, https://doi.org/10.21273/jashs.113.2.242.

[49] A.G. Quentin, A.P. O'Grady, C.L. Beadle, D. Worledge, E.A. Pinkard, Responses of transpiration and canopy conductance to partial defoliation of *Eucalyptus globulus* trees, Agr. For. Meterol. 151 (3) (2011) 356–364, https://doi.org/10.1016/j.agrformet.2010.11.008.

[50] V. Hernandez-Santana, J. Martínez-Fernandez, C. Moran, A. Cano, Response of *Quercus pyrenaica* (melojo oak) to soil water deficit: a case study in Spain, Eur. J. Forest Res. 127 (2008) 369–378, https://doi.org/10.1007/s10342-008-0214-x.

[51] J. Girona, M. Mata, D.A. Goldhamer, R.S. Johnson, T.M. DeJong, Patterns of soil and tree water status and leaf functioning during regulated deficit irrigation scheduling in peach, J. Am. Soc. Hortic. Sci. 118 (1993) 580–586, https://doi.org/10.21273/jashs.118.5.580.

[52] J.E. Schmidt, A.C.M. Gaudin, Toward an integrated root ideotype for irrigated systems, Trends. Plant Sci. 22 (5) (2017) 433–443, https://doi.org/10.1016/j.tplants.2017.02.001.

[53] T. Améglio, P. Archerd, M. Cohen, C. Valancogne, F.A. Audet, S. Dayau, P. Cruiziat, Significance and limits in the use of predawn leaf water potential for tree irrigation, Plant Soil. 207 (1999) 155–167, https://doi.org/10.10123/A:1026415302759.

[54] J.R. Ehleringer, C.S. Cook, Photosynthesis in Encelia farinosa Gray in Response to Decreasing Leaf Water Potential, Plant Physiol. 75 (3) (1984) 688–693, https://doi.org/10.1104/pp.75.3.688.

[55] R.S. Nowak, J.E. Anderson, N.L. Toft, Gas exchange of *Agropyron desertorum*: diurnal patterns and responses to water vapor gradient and temperature, Oecologia 77 (1988) 289–295, https://doi.org/10.1007/BF00378032.

[56] N. Nursultanov, C. Altaner, W.J.B. Heffernan, Effect of temperature on electrical conductivity of green sapwood of *Pinus radiata* (radiata pine), Wood. Sci. Technol. 51 (2017) 795–809, https://doi.org/10.1007/s00226-017-0917-6.

[57] L.V. Stott, B. Black, B. Bugbee, Quantifying Tree Hydration Using Electromagnetic Sensors, Horticulturae 6 (1) (2020) 2, https://doi.org/10.3390/horticulturae6010002.

[58] R.M. Rivero, M. Kojima, A. Gepstein, H. Sakakibara, R. Mittler, S. Gepstein, E. Blumwald, Delayed leaf senescence induces extreme drought tolerance in a flowering plant, Proc. Natl. Acad. Sci. U. S. A. 104 (49) (2007) 19631–19636, https://doi.org/10.1073/pnas.0709453104.

[59] A. Torrecillas, J.J. Alarcón, R. Domingo, J. Planes, M.J. Sánchez-Blanco, Strategies for drought resistance in leaves of two almond cultivars, Plant Sci. 118 (1996) 135–143, https://doi.org/10.1016/0168-9452(96)04434-2.

[60] C.D. Mellisho, N.Z. Cruz, W. Conejero, M.F. Ortuño, P. Rodriguez, Mechanisms for drought resistance in early maturing cv. Flordastar peach trees, J. Agric. Sci. 149 (2011) 609–616, https://doi.org/10.1017/S0021859611000141.

[61] M.C. Ruiz-Sánchez, R. Domingo, A. Torrecillas, A. Pérez-Pastor, Water stress preconditioning to improve drought resistance in young apricot plants, Plant Sci. 156 (2000) 245–251, https://doi.org/10.1016/s0168-9452(00)00262-4.

[62] R.W. Farebrother, Adrien-marie legendre (eds), in: C.C. Heyde, E. Seneta (Eds.), Statisticians of the Centuries, Springer, New York, 2001, pp. 101–104, 2001ISBN: 978-0-387-95283-3.